Controllability of the Vagus Nerve Using Directed Electrode Stimulation

Brianna Jacobson[1,2], Alice Ding[1,2], Ma Luo[1,2], Kyvia Pereira[1,2], Michael Miga[1,2,3,4,5]
[1]Vanderbilt Institute for Surgery and Engineering, Nashville, TN USA
[2]Vanderbilt University, Department of Biomedical Engineering, Nashville, TN USA
[3]Vanderbilt University Medical Center, Department of Radiology and Radiological Sciences, Nashville, TN USA
[4]Vanderbilt University Medical Center, Department of Neurological Surgery, Nashville, TN USA
[5]Vanderbilt University Medical Center, Department of Otolaryngology – Head and Neck Surgery, Nashville, TN USA

Abstract

Vagus nerve stimulation (VNS), commonly used to reduce seizures in patients with epilepsy, is a promising therapeutic treatment for a number of health issues. Current VNS apparatuses employ a helical electrode design, which stimulates the nerve with no anatomical specificity. The efficacy and breadth of VNS therapy could be improved by targeting stimulation to specific regions of the nerve. A mock electrode was built around a morphologically accurate finite element model of the vagus nerve. Electric currents were injected into the nerve model, and a nodal activating function was used to determine which axons would initiate action potentials. Electrode configurations and stimulation settings were adjusted to target specific fascicles until optimal activation was achieved. Results indicated that small, proximal electrodes could stimulate targeted regions while avoiding activation of off-target axons. Injection of negative current perpendicular to the positive stimulus also proved to refine spatial stimulation, allowing for the activation of deep fascicles with minimal side-effects. While an understanding of the fascicular anatomy of the vagus nerve is still being explored, the preliminary results of this study corroborate the concept of selectively targeting regions of the nerve with electrical stimulation in order to treat specific patient needs. The computational process presented in this work could be employed as a planning tool prior to the geometrical design and surgical implantation of VNS devices.

Keywords: vagus nerve, fascicular anatomy, neuromodulation, finite element modeling, selective stimulation

Introduction

The vagus nerve (VN) connects many of the body's organs to the brain and controls a vast array of physiological functions. It is the largest and longest connection between the peripheral and central nervous systems [4], and it is, therefore, one of the most promising targets for neuromodulation. Vagus Nerve Stimulation (VNS) was FDA approved in 1997 as a therapy for drug-resistant epilepsy and later, in 2005, as a treatment-resistant depression [23]. Since its emergence, VNS devices have successfully been implanted in more than 100,000 patients [28].

Given the vagus nerve's central role in autonomic nervous system function, VNS is being explored as a potential treatment for a variety of inflammatory disorders, including cardiovascular disease, respiratory issues, irritable bowel syndrome, sepsis, chronic pain, obesity, diabetes, and rheumatoid arthritis [5, 6, 18]. There have been promising pre-clinical and clinical results using VNS to reduce symptoms and slow loss-of-cognition associated with neurodegenerative disorders including Alzheimer's and Parkinson's [7, 12, 19]. The potential applications of neuromodulation is driving the research and development of better VNS devices and stimulation techniques.

The prevalence of adverse side effects, however, is the motivation for improving VNS devices. Laryngeal side effects include cough, dyspnea, paresthesia, pain and voice alteration [1, 3]. Stimulation can also cause cardiopulmonary symptoms, such as bradycardia and bradypnea [26]. These complications result from stimulating the entire VN rather than selectively targeting the fibers responsible for modulating a particular physiological function [2].

Selective stimulation of the VN could have more effective therapeutic effects while minimizing collateral symptoms. Two mechanisms of selective VNS have emerged in recent years: fiber-selective and spatially-selective VNS [13]. Fiber selective stimulation utilizes the varied activation thresholds of different fiber types to precisely target axons of physiologic interest, whereas spatially selective stimulation targets specific regions within the nerve. A number of experiments have been conducted on fiber selective VNS [10, 22], while research on spatially specific VNS is limited, because the functional anatomy of the VN is still not well understood [30]. If the anatomy of the vagus nerve is functionally organized, stimulation could be directed to activate only the particular fascicles of interest [24].

In this work, stimulation levels, amount of current injected and electrode configuration are investigated to determine the extent to which activation of the vagus nerve can be controlled. A simple quantitative method to optimize fascicular activation is also suggested.

Methods

1. Finite Element Nerve/Electrode Model

A three-dimensional finite element model (FEM) of the vagus nerve was generated using COMSOL Multiphysics® [9]. The nerve was constructed to be 3 mm in diameter, consistent with cadaveric findings [15], and morphologically accurate based on histological images [25]. The nerve consisted of 12 fascicles of varying shapes and diameters embedded in epineurial connective tissue. Each fascicle represents a bundle of axons in endoneurial connective tissue.

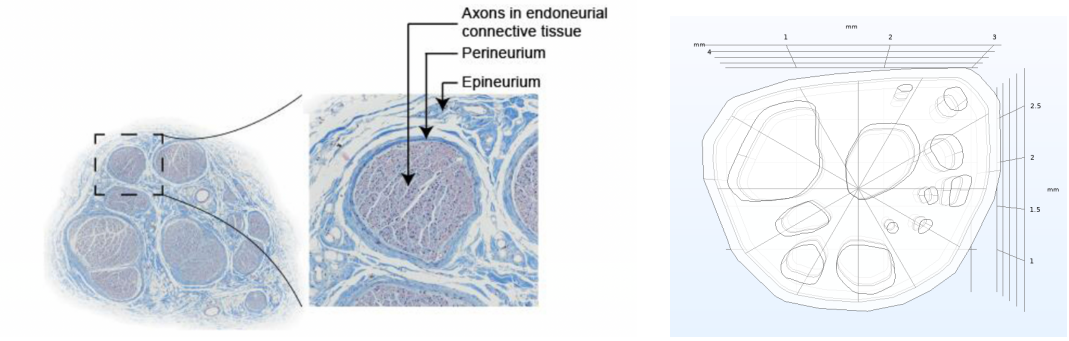

Figure 1: COMSOL model (right) based upon histological images of vagus nerve [25] (left).

The entire nerve was encompassed in a cylinder representing the carotid space, with the outer surface serving as the electrical ground. The domains of the nerve were assigned electrical properties (**Table 1**) consistent with human endoneurial, epineural and adipose tissue.

Table 1: Geometric and Electrical Properties of Nerve Model [14, 25]

Domain	Endoneurium	Epineurium	Adipose Tissue	Platinum
Electrical Conductivity (*S/m*)	.0833	.159	.0432	107
Relative Permittivity	21600	21600	393	1

A mock electrode design of 12 equally sized sectors was constructed around the circumference of the nerve out of platinum. Current could be injected into the nerve by 'activating' any combination of the electrode segments as a current source 'terminal'.

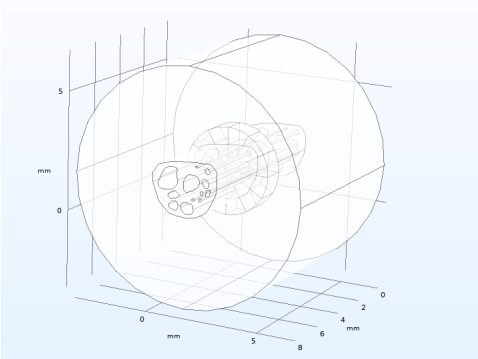

Figure 2: Entire 3D COMSOL model of nerve enclosed in 12-sectored electrode encased by layer of adipose tissue, serving as electrical ground.

The length of the nerve model was limited to 8 mm to reduce computation time. The boundary conditions were analyzed to confirm that the abbreviated length did not affect the electric distributions of interest. A tetrahedral mesh was generated consisting of 239,289 elements and 41,096 nodes.

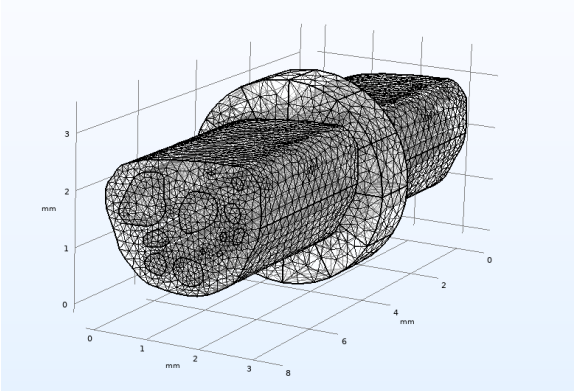

Figure 3: Generated tetrahedral mesh for nerve and segmented electrode (surrounding fat omitted for clarity).

Currents ranging from -2.0 mA up to 6.5 mA were injected into the nerve via various electrode configurations. The resulting electric potential distributions were then calculated in a stationary (steady-state) study by solving Poisson's equation.

2. Calculating Action Potentials

The voltage data from COMSOL was interpolated onto a three-dimensional grid constructed in accordance with the geometry of the nerve. Only points within fascicles were considered, with each longitudinal row of points representing nodes of Ranvier along a single axon fiber. Axons were spaced 0.1 mm apart in the cross-sectional direction, and nodes were spaced 0.5 mm apart along each axon, in accordance with a fiber diameter of 5.7 μm [21].

Based on the electric potential data from the model, the following activation function [29] was used to calculate the input current I(x) (mA) to each node along each axon:

$$I(x) = \frac{d}{4p_i c_m} \cdot \frac{\delta^2 V_e}{\delta x^2}$$

where d is the diameter of the axon fiber (μm), p_i is axoplasmic resistivity (Ω cm), c_m is capacitance of the node (μF/cm^2), V_e is extracellular voltage (V), and x is position along the axon (mm). For this study, axons

assumed a diameter of 5.7 μm, resistivity of 70 Ω cm, and capacitance of 2 μF/cm^2 [21].

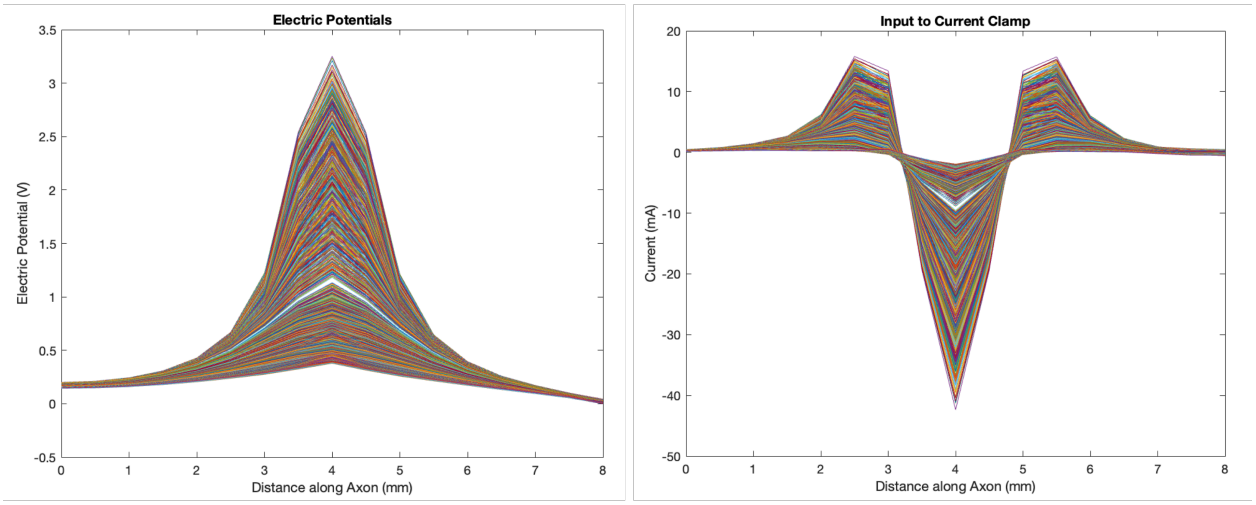

Figure 4: Electric potential (V) (left) and current clamp input (mA) (right) versus the position (mm) of each node along an axon for 2.00 mA of injected current via two electrode segments. Each color represents a single nerve fiber.

NEURON 5.7 [16] was utilized to simulate stimulation of axons in the nerve using the Hodgkin-Huxley excitation model [17]. The calculated currents were applied as a clamp input current to each node of Ranvier with a standard pulse width of 500 μs [20]. At each node, if the resulting membrane potential exceeded the threshold potential value, an action potential was assumed to be initiated. Since action potentials propagate down axons in an all-or-none fashion [27], if any node along an axon was activated, the entire axon was considered activated.

3. Targeting Specific Fascicles

To understand the controllability of VNS, separate studies were conducted with varying electrode configurations targeting different fascicles. The nerve model was stimulated over a range of input currents and action potentials were calculated using the method described above. The percentage of the intended region of the nerve that was activated (E) relays the efficacy of the model. An efficacy value of one (unity) represents total activation of the target fascicle(s), as shown in **Figure 5**. The percentage of the unintended region of the nerve that was activated (S) represents potential side-effect causing regions. The following objective function was used to evaluate the effectiveness of the stimulation:

$$f = E \times (1 - S)$$

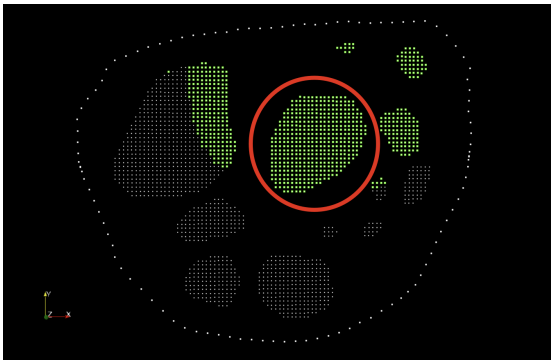

Figure 5: Example use of objective function. For the circled target fascicle, 100% of the target fascicle (E = 1.00) and 18.99% of the non-target axons (S = .1899) are activated, for an output value of f= (1.00)*(1-.1899) = .8101.

The maximum value of the objective function is achieved by total activation of the target fascicle(s) and zero activation of side-effect regions. The goal was to determine the amount of current needed to inject into the nerve in order to optimize the objective function to unity for any given target region.

Results

1. Effect of Current Amplitude on Nerve Activation

All twelve electrode segments were activated to impart total circumferential stimulation. Amplitude of injected current was increased until total activation of the nerve was achieved. In accordance with expectations and previous findings [11], neural activation appeared to increase linearly with increasing current stimulation.

Current Amplitude (mA)	Percent Activation
2.00	0.0349
3.00	0.3949
4.00	0.6394
5.00	0.9365
5.25	1

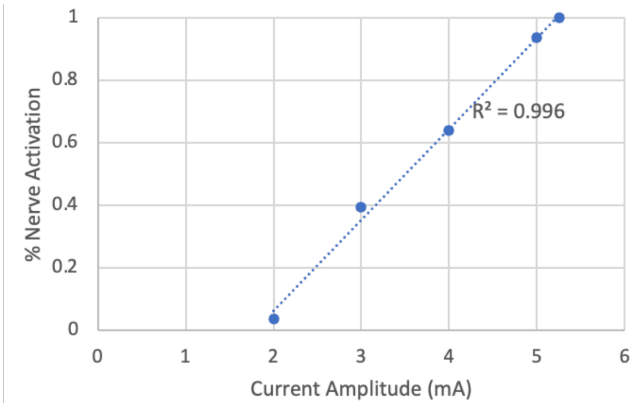

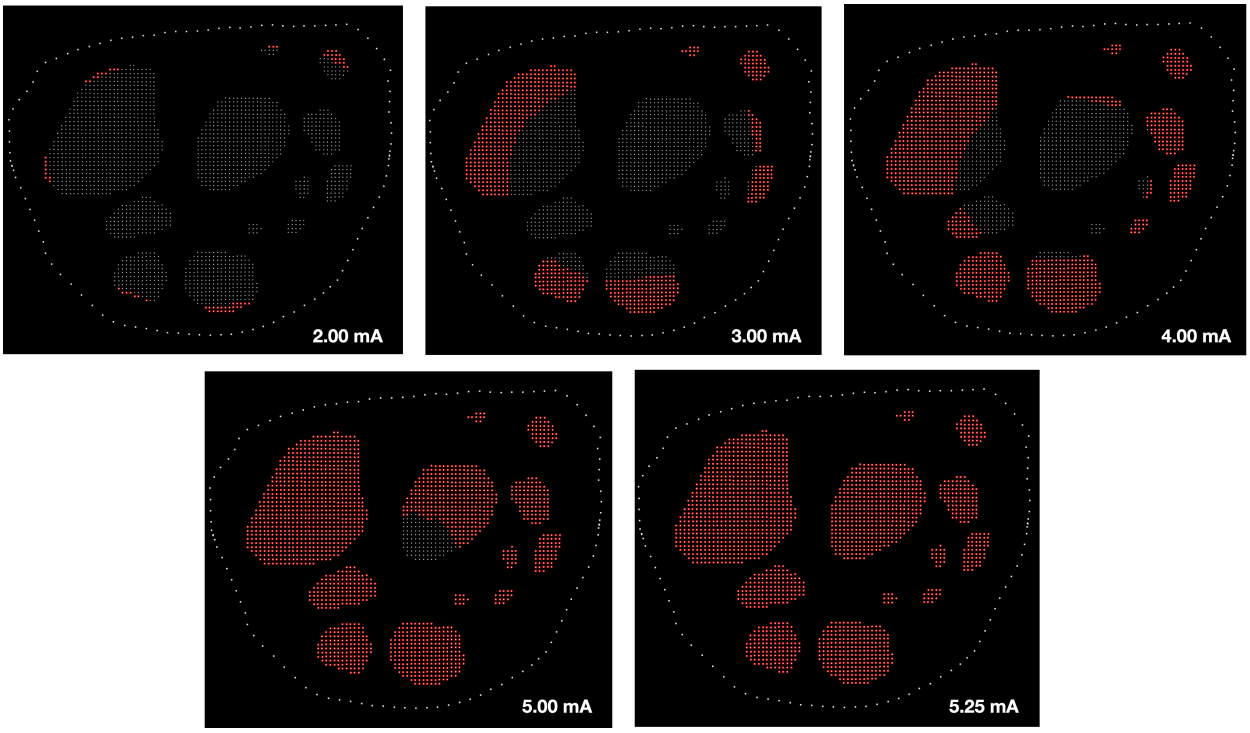

Figure 6: Increasing amplitude of stimulation via all twelve electrode segments until all axons activated. Percent nerve activation increased linearly (R^2 = .996) with increasing amplitude of injected current.

2. Effect of Surface Area of Stimulation on Nerve Activation

Activating more electrode segments did not necessarily increase neural activation. At 2.00 mA of stimulation, turning on all twelve electrode segments activated only 3.49% of the entire nerve, where as just two electrode segments were able to activate 33.71% of the neural fibers. Recall that the input clamp current at each node of Ranvier is proportional to the second derivative of the extracellular electric potential induced by the electrodes.

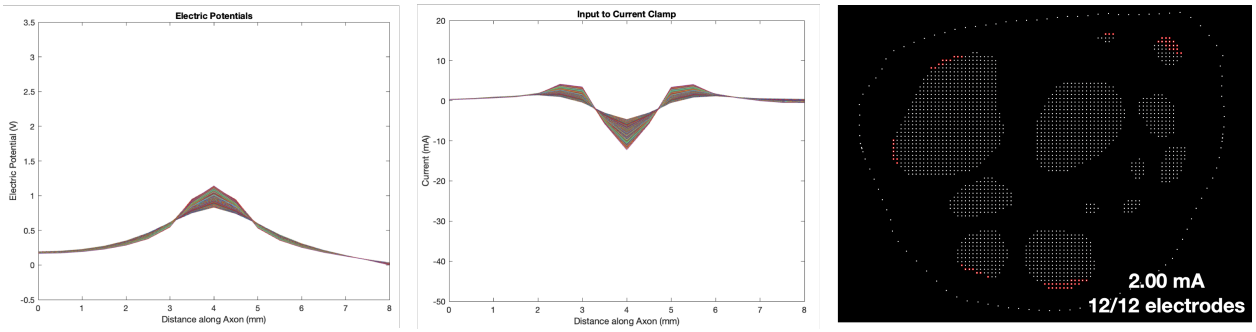

Figure 7a: 2.00 mA of injected current via all twelve electrodes. Electric potential (V) (left) and current clamp input (mA) (middle) versus the position (mm) of each node along an axon. Resulting region of activation is shown in red, spanning 3.49% of the entire nerve (right).

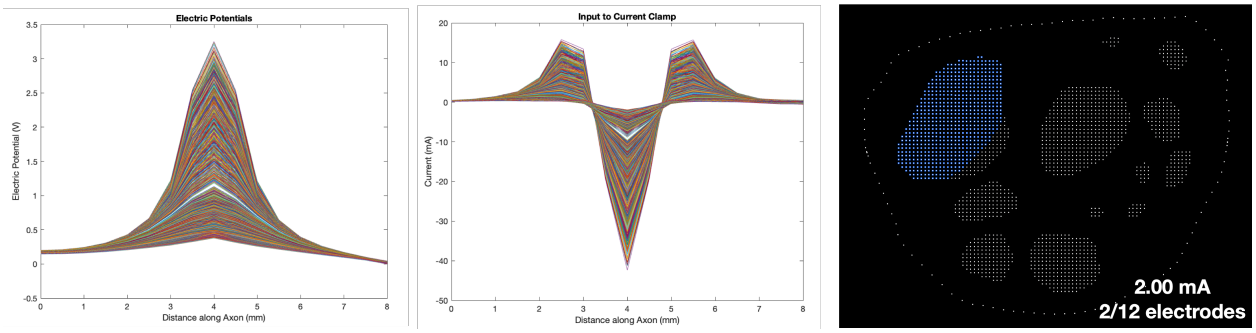

Figure 7b: 2.00 mA of injected current via only two electrodes. Electric potential (V) (left) and current clamp input (mA) (middle) versus the position (mm) of each node along an axon. Resulting region of activation is shown in blue, spanning 33.71% of the entire nerve (right).

3. Effect of Electrode Configuration on Nerve Activation

Several unique electrode configurations were tested to target particular fascicles in the model. Given that neural activation increases with current, the amplitude of the applied current stimulus was increased until maximum activation of the targeted fascicle was achieved. Fascicles close to the perineurial surface were easily targeted by activating the nearest electrode segment(s) without incurring significant side effects.

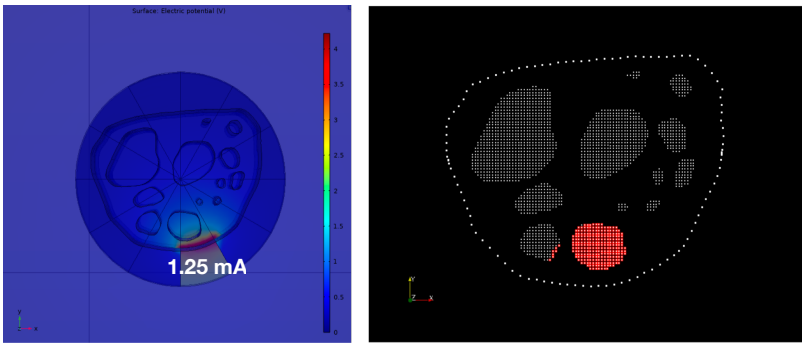

Figure 8a: Single nearest electrode activated (left) and resulting activation of target fascicle shown in red (right). Optimal fascicle activation (E = .9960, S = .0036, f = .9924) was achieved at injected current amplitude of 1.25 mA.

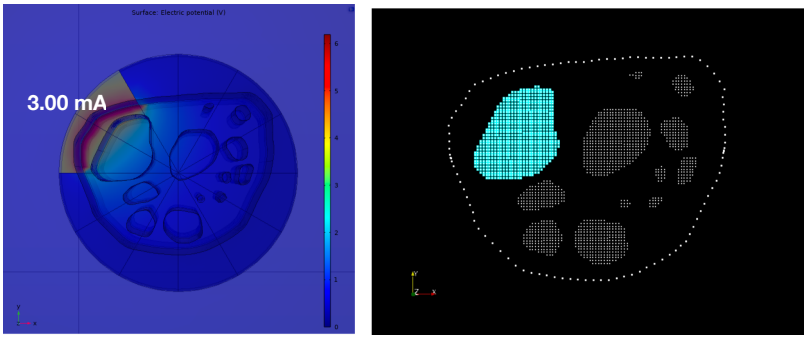

Figure 8b: Two nearest electrodes activated (left) and resulting activation of target fascicle shown in blue (right). Optimal fascicle activation (E = 1, S = 0, f = 1) was achieved at injected current amplitude of 3.00 mA.

Fascicles located more centrally within the nerve were less accessible to the surface electrodes. Activation of the nearest electrode to deep fascicles induced significant side effects. Injection of negative current from other electrodes counteracted stimulation to mitigate side effects in non-target fascicles.

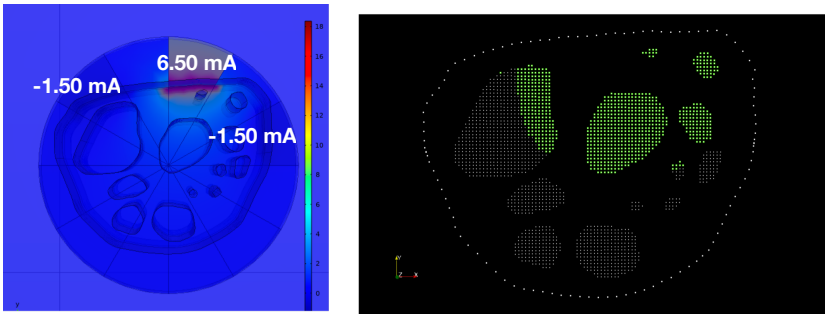

Figure 9: Combination of positive (red boundary) and negative (dark blue boundaries) stimulation (left) and resulting activation of central fascicle shown in green (right). Optimal fascicle activation (E = 1, S = .1899, f = .8101) was achieved at injected current amplitude of 6.50 mA via the positive electrode and -1.50 mA via the two negative electrodes.

Discussion

The results of this study show how electrical stimulation can be engineered to target specific regions of interest within the vagus nerve. The number of axons that are activated can be controlled by varying the amount of current stimulation (**Figure 6**). Increasing the amplitude of stimulation increases axonal recruitment.

The typical helical electrode design, which wraps 270° around the circumference of the nerve, lacks spatial specificity and is not the most effective configuration for neural activation. This work investigated a multi-contact array of smaller electrodes as a potential alternative solution. With equivalent levels of current stimulation, the segmented electrode design in contact with only portions of the nerve surface is more effective at axonal recruitment than the helical geometry (**Figure 7**). This finding can be attributed to the asymmetry of the stimulation, which induces a larger gradient in electric potential than a symmetrical arrangement, in turn recruiting a larger number of axons. Other anatomical models have corroborated the improved therapeutic efficacy of flat electrode contacts [8] and multielectrode arrays [2].

Electrode configuration was the most influential factor on neural activation. It was observed that electrode surfaces tend to activate the nearest axons. VNS can be controlled to target specific fascicles by injecting a current at the nearest portion of the nerve surface (**Figure 8**). Stimulation can be directed at fascicles located deep within a nerve by activating the nerve surface proximally to the target region and injecting negative perpendicularly to counteract activation of side effects regions (**Figure 9**). By controlling the amplitude of current stimulation and the geometry of electrodes, specific fascicles within the VN can be targeted.

Conclusion

Vagus nerve stimulation has a vast array of potential therapeutic applications. Therapeutic efficacy and applicability would be improved if generation of side-effects can be avoided. Directed electrode stimulation is an alternative to traditional VNS technology and potential treatment for patient-specific inflammatory symptoms. This work provides a pathway to optimize the efficacy of nerve stimulation. Using the computational model, a multi-contact electrode design can be calibrated to activate specific regions of the vagus nerve while avoiding generation of off-target effects. The plausible controllability of fascicular activation has promising implications for VNS, pending further exploration of the so-called 'vagotopy' [30] and fabrication of a functional segmented electrode device.

Acknowledgements

This work is supported in part by the National Institutes of Health, the National Institute for Neurological Disorders and Stroke, R01NS049251. This work is also supported by the Vanderbilt Institute for Surgery and Engineering Summer Undergraduate Research Fellow Program.

References

1. Al Omari, A. I., Alzoubi, F. Q., Alsalem, M. M., Aburahma, S. K., Mardini, D. T., & Castellanos, P. F. (2017). The vagal nerve stimulation outcome, and laryngeal effect: Otolaryngologists roles and perspective. *American journal of otolaryngology*, *38*(4), 408–413.

2. Aristovich, K., Donega, M., Fjordbakk, C., Tarotin, I., Chapman, C., Viscasillas, J., Stathopoulou, T. R., Crawford, A., Chew, D., Perkins, J., & Holder, D. (2021). Model-based geometrical optimisation and in vivo validation of a spatially selective multielectrode cuff array for vagus nerve neuromodulation. *Journal of neuroscience methods*, *352*, 109079.

3. Ben-Menachem, E., Revesz, D., Simon, B. J., and Silberstein, S. (2015). Surgically implanted and non-invasive vagus nerve stimulation: a review of efficacy, safety and tolerability. *Eur. J. Neurol.* 22, 1260–1268.

4. Berthoud, H. R., & Neuhuber, W. L. (2000). Functional and chemical anatomy of the afferent vagal system. *Autonomic neuroscience : basic & clinical*, *85*(1-3), 1–17.

5. Bonaz, B., Sinniger, V., & Pellissier, S. (2016). Anti-inflammatory properties of the vagus nerve: potential therapeutic implications of vagus nerve stimulation. *The Journal of physiology*, *594*(20), 5781–5790.

6. Breit, S., Kupferberg, A., Rogler, G., & Hasler, G. (2018). Vagus Nerve as Modulator of the Brain-Gut Axis in Psychiatric and Inflammatory Disorders. *Frontiers in psychiatry*, *9*, 44.

7. Broncel, A., Bocian, R., Kłos-Wojtczak, P., Kulbat-Warycha, K., & Konopacki, J. (2020). Vagal nerve stimulation as a promising tool in the improvement of cognitive disorders. *Brain research bulletin*, *155*, 37–47.

8. Bucksot, J. E., Wells, A. J., Rahebi, K. C., Sivaji, V., Romero-Ortega, M., Kilgard, M. P., Rennaker, R. L., 2nd, & Hays, S. A. (2019). Flat electrode contacts for vagus nerve stimulation. *PloS one*, *14*(11), e0215191.

9. COMSOL Multiphysics® v. 5.4. www.comsol.com. COMSOL AB, Stockholm, Sweden.

10. Dali, M., Rossel, O., Andreu, D., Laporte, L., Hernández, A., Laforet, J., Marijon, E., Hagège, A., Clerc, M., Henry, C., & Guiraud, D. (2018). Model based optimal multipolar stimulation without a priori knowledge of nerve structure: application to vagus nerve stimulation. *Journal of neural engineering*, *15*(4), 046018.

11. Ding, A. K., Luo, M., Miga, M. I. (2021). Modeling the effects of bipolar helical cuff electrodes in vagus nerve stimulation. *Proc. SPIE, Medical Imaging 2021: Image-Guided Procedures, Robotic Interventions, and Modeling*, 115982H.

12. Farrand, A. Q., Helke, K. L., Gregory, R. A., Gooz, M., Hinson, V. K., & Boger, H. A. (2017). Vagus nerve stimulation improves locomotion and neuronal populations in a model of Parkinson's disease. *Brain stimulation*, *10*(6), 1045–1054.

13. Fitchett, A., Mastitskaya, S., & Aristovich, K. (2021). Selective Neuromodulation of the Vagus Nerve. *Frontiers in neuroscience*, *15*, 685872.

14. Grill, W. M., & Mortimer, J. T. (1994). Electrical properties of implant encapsulation tissue. *Annals of biomedical engineering*, *22*(1), 23–33.

15. Hammer, N., Löffler, S., Cakmak, Y. O., Ondruschka, B., Planitzer, U., Schultz, M., Winkler, D., & Weise, D. (2018). Cervical vagus nerve morphometry and vascularity in the context of nerve stimulation - A cadaveric study. *Scientific reports*, *8*(1), 7997.

16. Hines, M. L., & Carnevale, N. T. (2001). NEURON: a tool for neuroscientists. *The Neuroscientist: a review journal bringing neurobiology, neurology and psychiatry*, *7*(2), 123–135.

17. Hodgkin, A. L., & Huxley, A. F. (1952). A quantitative description of membrane current and its application to conduction and excitation in nerve. *The Journal of physiology*, *117*(4), 500–544.

18. Johnson, R. L., & Wilson, C. G. (2018). A review of vagus nerve stimulation as a therapeutic intervention. *Journal of inflammation research*, *11*, 203–213.

19. Kin, I., Sasaki, T., Yasuhara, T., Kameda, M., Agari, T., Okazaki, M., Hosomoto, K., Okazaki, Y., Yabuno, S., Kawauchi, S., Kuwahara, K., Morimoto, J., Kin, K., Umakoshi, M., Tomita, Y., Tajiri, N., Borlongan, C. V., & Date, I. (2021). Vagus Nerve Stimulation with Mild Stimulation Intensity Exerts Anti-Inflammatory and Neuroprotective Effects in Parkinson's Disease Model Rats. *Biomedicines*, *9*(7), 789.

20. Labiner, D. M., & Ahern, G. L. (2007). Vagus nerve stimulation therapy in depression and epilepsy: therapeutic parameter settings. *Acta neurologica Scandinavica*, *115*(1), 23–33.

21. McIntyre, C. C., Richardson, A. G., & Grill, W. M. (2002). Modeling the excitability of mammalian nerve fibers: influence of afterpotentials on the recovery cycle. *Journal of neurophysiology*, *87*(2), 995–1006.

22. McAllen, R. M., Shafton, A. D., Bratton, B. O., Trevaks, D., & Furness, J. B. (2018). Calibration of thresholds for functional engagement of vagal A, B and C fiber groups *in vivo*. *Bioelectronics in medicine*, *1*(1), 21–27.

23. McLachlan R. S. (1997). Vagus nerve stimulation for intractable epilepsy: a review. *Journal of clinical neurophysiology : official publication of the American Electroencephalographic Society*, *14*(5), 358–368.

24. Nicolai, E. N., Settell, M. L., Knudsen, B. E., McConico, A. L., Gosink, B. A., Trevathan, J. K., Baumgart, I. W., Ross, E. K., Pelot, N. A., Grill, W. M., Gustafson, K. J., Shoffstall, A. J., Williams, J. C., & Ludwig, K. A. (2020). Sources of off-target effects of vagus nerve stimulation using the helical clinical lead in domestic pigs. *Journal of neural engineering*, *17*(4), 046017.

25. Pelot, N. A., Behrend, C. E., & Grill, W. M. (2019). On the parameters used in finite element modeling of compound peripheral nerves. *Journal of neural engineering*, *16*(1), 016007.

26. Plachta, D. T., Gierthmuehlen, M., Cota, O., Espinosa, N., Boeser, F., Herrera, T. C., Stieglitz, T., & Zentner, J. (2014). Blood pressure control with selective vagal nerve stimulation and minimal side effects. *Journal of neural engineering*, *11*(3), 036011.

27. Platkiewicz, J., & Brette, R. (2010). A threshold equation for action potential initiation. *PLoS computational biology*, *6*(7), e1000850.

28. Purser, M. F., Mladsi, D. M., Beckman, A., Barion, F., & Forsey, J. (2018). Expected Budget Impact and Health Outcomes of Expanded Use of Vagus Nerve Stimulation Therapy for Drug-Resistant Epilepsy. *Advances in therapy*, *35*(10), 1686–1696.

29. Rattay F. (1999). The basic mechanism for the electrical stimulation of the nervous system. *Neuroscience*, *89*(2), 335–346.

30. Settell, M. L., Pelot, N. A., Knudsen, B. E., Dingle, A. M., McConico, A. L., Nicolai, E. N., Trevathan, J. K., Ezzell, J. A., Ross, E. K., Gustafson, K. J., Shoffstall, A. J., Williams, J. C., Zeng, W., Poore, S. O., Populin, L. C., Suminski, A. J., Grill, W. M., & Ludwig, K. A. (2020). Functional vagotopy in the cervical vagus nerve of the domestic pig: implications for the study of vagus nerve stimulation. *Journal of neural engineering*, *17*(2), 026022.